



Numerical investigations of tsunamis generated by pyroclastic flows from the Kikai caldera, Japan

Fukashi Maeno¹ and Fumihiko Imamura²

Received 4 July 2007; revised 23 October 2007; accepted 31 October 2007; published 6 December 2007.

[1] Tsunamis generated by a voluminous pyroclastic flow entering the sea during a caldera-forming eruption at the Kikai caldera, Japan, were investigated by using a two-layer shallow water model which is limited to the source conditions and their impact on coastal areas. Volume flux of the dense component of the pyroclastic flow was controlled by a sine function. Results showed that the maximum height of the tsunami was largest in models with the largest volume flux of the flows. The approximate source conditions of the tsunami, which can stir sediment particles on the sea floor, were investigated using the non-dimensional boundary shear stress. Results from our simulation showed that the shear stress to initiate movement of sediment particles was not easily achieved in areas where there was evidence of a tsunami. A caldera collapse is thought more likely to have generated the huge tsunami rather than a pyroclastic flow. **Citation:** Maeno, F., and F. Imamura (2007), Numerical investigations of tsunamis generated by pyroclastic flows from the Kikai caldera, Japan, *Geophys. Res. Lett.*, 34, L23303, doi:10.1029/2007GL031222.

1. Introduction

[2] Tsunamis generated by explosive caldera-forming eruptions in shallow seas can cause serious damage to coastal areas [Cas and Wright, 1991; Beget, 2000]. One possible mechanism for the generation of a destructive tsunami is the sudden entrance of pyroclastic flows into the sea. The result is a rapid transfer of flow momentum into seawater [e.g., Watts and Waythomas, 2003] that transmits the damaging effects of an eruption over large distances. This was seen in the 1883 Krakatau eruption and the 3.6 ka Santorini eruption [Carey et al., 1996; McCoy and Heiken, 2000].

[3] The 7.3 ka eruption of the Kikai caldera (Figure 1), the largest and most notable caldera-forming eruption in Japan during the Holocene [Machida and Arai, 1978], occurred in a shallow sea and was of larger scale (Volcano explosive index, VEI, is 7) than the Santorini or Krakatau eruptions (VEI \cong 6). A relationship was recently established between tsunamis generated by a caldera collapse and the respective eruption scale using simple plunger models with shallow water wave equations and a hypothetical caldera collapse scale [Maeno et al., 2006]. However, the conditions of a voluminous pyroclastic flow entering the sea and the impact remain to be studied in detail.

[4] In this paper, the impact of a large volume pyroclastic flow entering the sea during the 7.3 ka Kikai eruption was

simulated numerically using a two-layer shallow-water model derived from the full set of Euler equations [Imamura and Imteaz, 1996] and geological data [Maeno and Taniguchi, 2007]. Although the aerial part of the pyroclast flowed across the sea surface, we assumed that a major impact was caused by a dense debris component flowing down to the seafloor. The behavior and scale of tsunamis, controlled by volume, mass flux, and duration time of the pyroclastic flow, are discussed. The results are compared with those from caldera collapse models [Maeno et al., 2006].

[5] The distribution of submarine deposits in the Kikai eruption has not been fully investigated, but the deposits around the Kikai caldera have been roughly surveyed by the *Japan Coast Guard* [1982]. The submarine deposits are leanly distributed to the north and south-west of the caldera with more than 3 km³ total volume and up to 60 m thick. These deposits may have been derived from the submarine component of a huge pyroclastic flow. Critical evidence of tsunami generation in the 7.3 ka eruption was recently found in submarine sediments in Tachibana Bay, 220 km far from the source, located on the western coast of Kyushu. Okamura et al. [2005] found sand layers, including granule- or pebble-size well-rounded grains and shell fragments, about 20 cm thick. The layers underlie the 7.3 ka cognimbrite ash layer in two piston cores recovered from the central part of the Bay. They interpreted that the Kikai eruption caused a huge tsunami that washed out the coastal area of Tachibana Bay.

2. Numerical Model

[6] In our model, it is assumed that a basal part of a pyroclastic flow is composed of materials that are denser than water and that it slides into the sea. In the simulation, a mathematical model for a two-layer flow in a wide channel with a non-horizontal bottom [Imamura and Imteaz, 1996] was used. The model assumes a hydrostatic pressure distribution, negligible interfacial mixing, as well as uniform density and velocity distributions in each layer. Considering the two-dimensional case, Euler equations of mass and momentum continuity are integrated in each layer, with the kinetic and dynamic conditions at the free surface and interface. The governing equations including full non-linearity under the assumption of long-wave approximation for the upper layer (tsunami) are given below (only x -direction):

$$\frac{\partial(\eta_1 - \eta_2)}{\partial t} + \frac{\partial M_1}{\partial x} + \frac{\partial N_1}{\partial y} = 0 \quad (1)$$

$$\frac{\partial M_1}{\partial t} + \frac{\partial}{\partial x} \left(\frac{M_1^2}{D_1} \right) + \frac{\partial}{\partial y} \left(\frac{M_1 N_1}{D_1} \right) + g D_1 \frac{\partial \eta_1}{\partial x} - INTF_x = 0 \quad (2)$$

¹Earthquake Research Institute, University of Tokyo, Tokyo, Japan.

²Disaster Control Research Center, Graduate School of Engineering, Tohoku University, Sendai, Japan.



Figure 1. (a) Location of the Kikai caldera, south of Kyushu, Japan. This map also shows the computed area used for the numerical simulations. Tsunami data were collected at four points (1: Makurazaki, 2: Ei, 3: Nejime, 4: Tachibana Bay). (b) In the numerical simulations, pyroclastic flows are generated from a circular source of 4 km radius in the center of the pre-caldera island.

and those for the lower layer (dense component of pyroclastic flow) are:

$$\frac{\partial \eta_2}{\partial t} + \frac{\partial M_2}{\partial x} + \frac{\partial N_2}{\partial y} = 0 \quad (3)$$

$$\begin{aligned} & \frac{\partial M_2}{\partial t} + \frac{\partial}{\partial x} \left(\frac{M_2^2}{D_2} \right) + \frac{\partial}{\partial y} \left(\frac{M_2 N_2}{D_2} \right) \\ & + g D_1 \left(\alpha \frac{\partial D_1}{\partial x} + \frac{\partial \eta_2}{\partial x} - \frac{\partial h_1}{\partial x} \right) \\ & + \frac{g n^2}{D_2^3} M \sqrt{M^2 + N^2} + \alpha INTF_x = DIFF_x \end{aligned} \quad (4)$$

where η is the water surface elevation, $D = h + \eta$ the total depth, h the still water depth, M (x -direction) and N (y -direction) the discharge, ρ the density of fluid, $\alpha = \rho_1/\rho_2$, g gravitational acceleration, n the bottom friction coefficient, $INTF$ the term of interfacial shear stress, $DIFF$ the term of horizontal diffusion force, and subscripts 1 and 2 indicate

the upper and lower layers, respectively. The stress terms are described by the equations (5) and (6) (only x -direction):

$$INTF_x = f_{inter} \bar{u} \sqrt{\bar{u}^2 + \bar{v}^2} \quad (5)$$

$$DIFF_x = \nu \sqrt{\frac{\partial^2 M}{\partial x^2} + \frac{\partial^2 M}{\partial y^2}} \quad (6)$$

where \bar{u} (x -direction) and \bar{v} (y -direction) are the depth-averaged tsunami velocity, f_{inter} the interfacial drag coefficient between density current and water, and ν the diffusion coefficient. The pyroclastic flow on a subaerial volcano can be calculated by the still water depth (h) being zero, that is, only the lower layer is simulated and no interaction between pyroclastic flow and sea water occurs. The artificial viscosity, which is described as $\beta(\Delta x)^3 \sqrt{g/D} |\partial^2 \eta / \partial x^2| |\partial^2 \eta / \partial y^2|$ where β is the constant, is also introduced into the mass conservation equation (equation 1) to control numerical instability.

3. Physical Conditions and Parameters of Pyroclastic Flow

[7] It is assumed that before the eruption an island existed at the present Kikai caldera (Figure 1). Such pre-eruptive geometry was also used in the tsunami simulations for a caldera collapse model [Maeno *et al.*, 2006]. It is also assumed that a dense component composed of mainly lithic (about 10 km³ [Maeno and Taniguchi, 2007]) was generated from a circular source of 4 km radius in the center of the island. The physical conditions of the flow are controlled by a volume flux (Q), prescribed as $Q = Q_{max} \sin(t\pi/T)$, where Q_{max} is maximum volume flux, t is time, and T is the duration of the eruption. The total volume of the dense flow and the duration time can be described as $V = \int Q dt$ and $T = \pi V / 2 Q_{max}$, respectively. All parameter values used in this study are listed in Table 1.

[8] The density of the basal component of the pyroclastic flow was assumed to be constant, 1250 kg/m³ ($\alpha = 0.8$), which is a plausible value for the basal boundary layer where grain concentration is high [e.g., Wohletz, 1998]. The turbulent diffusion and the interfacial drag coefficients between the pyroclastic flow and seawater are set to be 0.01 and 0.2, respectively, based on experimental studies of granular slides into water [Matsumoto *et al.*, 1998; Kawamata *et al.*, 2005]. The bottom friction coefficient, n , was set to be 0.01 for the subaerial flow and to be 0.08 for the submarine flow; based on comparisons between numerical results of this study and experimental results, which analogized pyroclastic flow entering sea in laboratories [e.g., McLeod *et al.*, 1999], with respect to time and distance plots of subaqueous density currents.

4. Conditions of the Numerical Calculations

[9] The non-linear long wave equations were discretized using the staggered leap-frog scheme with a truncation error of the second order, and the Courant, Friedrichs, and Lewy (CFL) condition was used in the calculations [Goto and Ogawa, 1992]. Computed sea levels were collected at 6 min

Table 1. Parameters for Numerical Calculations of a Pyroclastic Flow Entering the Sea^a

Models	Pyroclastic Flow			Tsunami			
	V , km ³	Q_{max} , m ³ /s	T , s	Location 1		Location 4	
				η_{max} , m	η_{max} , m	U_0 , m/s	U_s , m/s
Model 1a	10	1.0E+08	157	23	2.0	0.8	0.033
Model 1b	10	5.0E+07	314	15	1.7	0.7	0.029
Model 1c	10	2.0E+07	785	15	0.8	0.4	0.016
Model 1d	10	1.0E+07	1571	8	0.5	0.2	0.008
Model 2a	5	1.0E+08	79	17	1.5	0.7	0.029
Model 2b	5	5.0E+07	157	13	1.3	0.6	0.024
Model 2c	5	2.0E+07	393	11	0.8	0.4	0.016
Model 2d	5	1.0E+07	785	10	0.5	0.2	0.008
Model 3b	3	5.0E+07	94	11	0.9	0.4	0.016
Model 3c	3	2.0E+07	236	9	0.7	0.3	0.012
Model 3d	3	1.0E+07	471	8	0.5	0.2	0.008

^a Q_{max} , maximum volume flux; V , volume; T , duration; η_{max} , maximum wave height; U_0 , depth-averaged velocity; U_s , shear velocity. Duration of calculations is set to be 2.3 hours for all models.

intervals for the entire grid mesh. These procedures are the same as the ones used for caldera collapse models [Maeno et al., 2006]. For data in the computational domain, Δx , 150 m grid was used for all areas and all models. A time interval, Δt , was set to be 0.1 s during the pyroclastic flow entering sea, and to be 0.5 s after that to avoid numerical dissipation.

5. Results of Numerical Calculations

[10] Results of the numerical computations calculated from the relationship between the maximum volume flux, Q_{max} , and total volume of submarine pyroclastic flow, V , with each model (Table 1) showed that the maximum height of the tsunami around the caldera varies. The volume flux of the dense component of the pyroclastic flow can be com-

pared with the limiting flux of the water displacement, $h\sqrt{gh}$, which may strongly control wave amplitude [e.g., Walder et al., 2003]. Figures 2a–2d shows the relationship between the maximum height of the tsunami (η_{max}) at each location and the maximum volume flux (Q_{max}) with all models. The computed maximum height of the tsunami was the largest when the volume flux was the largest, 10^8 m³/s, for all models. In the simulations, the sea level rapidly rose just after the pyroclastic flow entered the sea as the flow displaced seawater toward the far area and seawater was dragged into the deeper part, resulting in tsunami generation with a positive leading wave. In models with a small volume flux, the effect of the interaction on the wave generation seemed weak.

[11] Numerical results using model 1a with the maximum volume flux are shown as an example (Figure 3), where the first positive peak reached Yaku-shima within 12 minutes, Satsuma Peninsula within 18 minutes, and Tane-ga-shima within 25 minutes. A typical waveform shows a positive peak followed by a negative one, which is the opposite of the waveform in caldera collapse models [Maeno et al., 2006]. Although the computed tsunami showed differences in maximum heights and arrival times with different volume flux, there were no significant differences in the shape of the waveforms with the same volume flux.

[12] At three locations along the coasts of the Kyushu mainland, the maximum height of the tsunami (Figures 2a–2d) and the factors controlling whether inundation occurs at those locations were investigated. In the results, the first positive waves in the larger volume flux models produced run-up on land. At Ei (location 2 in Figure 1), the primary wave inundated nearly 1 km inland and had a maximum height of more than 20 m for the largest volume flux model (models 1a and 2a). When the volume flux was lower, the tsunami height was drastically decreased to just a few meters and it did not produce inundation for most coastal areas. The approximate value of the maximum volume flux necessary to cause inundation was $2\sim 5 \times 10^7$ m³/s at

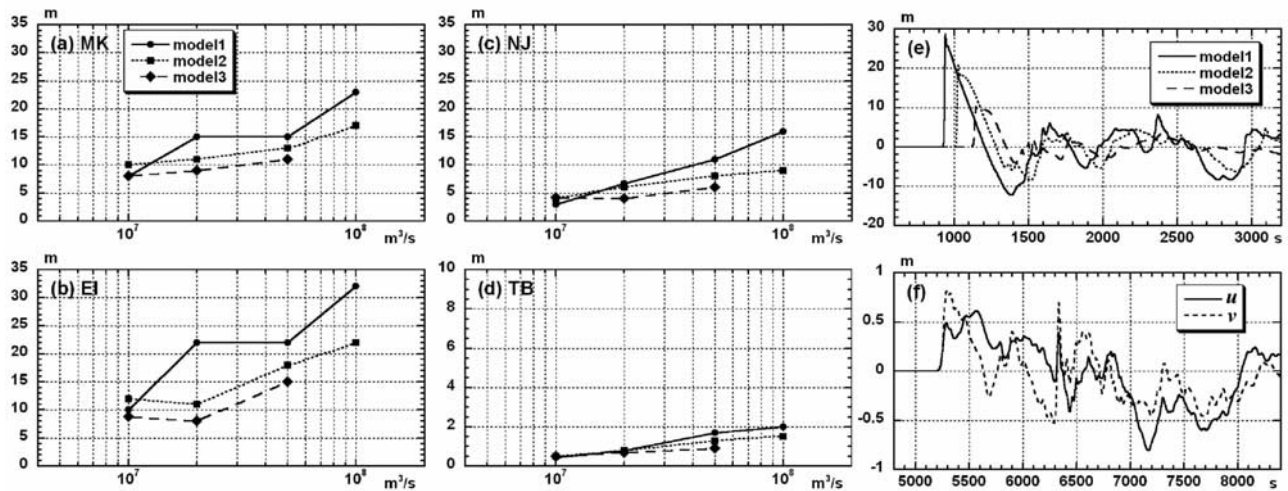


Figure 2. Computed maximum heights of the tsunami with all models at (a) Makurazaki, (b) Ei, (c) Nejime, and (d) Tachibana Bay. (e) Comparison of tsunami waveforms with different volume flux (models 1a, 1b, and 1c). Time in the abscissa is in seconds. The waveforms are computed at the Osumi Strait (See Figure 1). (f) Depth-averaged velocity of tsunami at Tachibana Bay. (u : x -direction; v : y -direction)

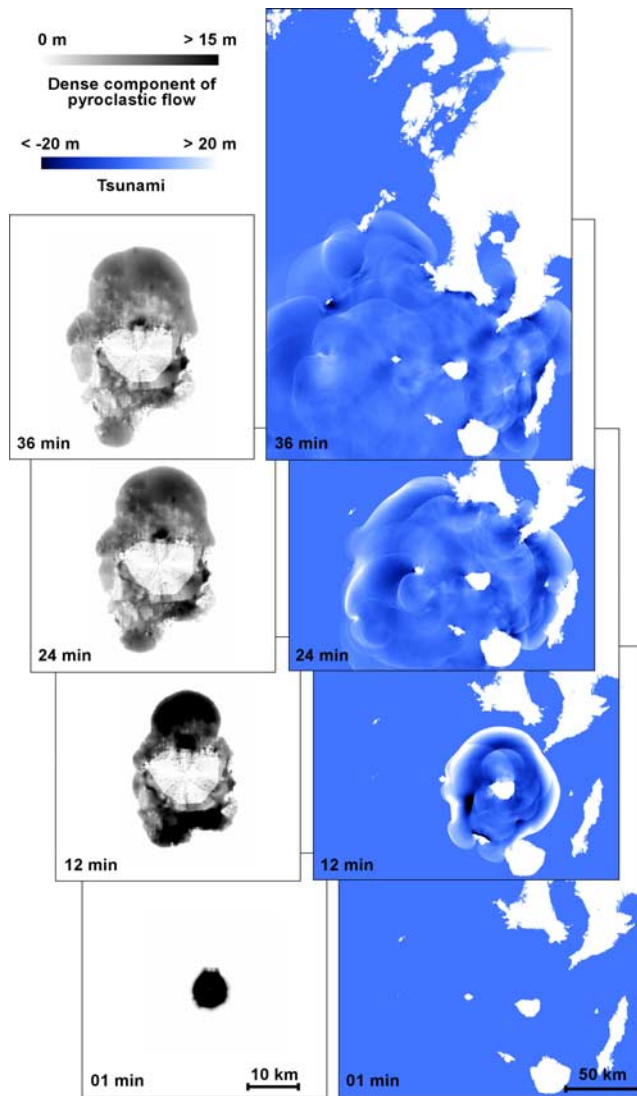


Figure 3. (left) Results of numerical calculations of the dense component of a pyroclastic flow entering the sea and (right) tsunami generation, using model 1a. Left-side figures are magnifications of the caldera area. Numbers in each figure show minutes from the start.

Makurazaki and Ei on the Satsuma Peninsula. At Nejime on the Osumi Peninsula (Figure 1), inundation did not occur for all models. In the far field, characteristics became less sensitive to the generation mechanisms. In Tachibana Bay, the maximum height of the tsunami was only 2.4 m even in model 1a.

6. Effects on Submarine Sediments and Comparisons With the Caldera-Collapse Model

[13] Geological evidence of tsunami generation and propagation during the 7.3 ka Kikai eruption exists in the submarine sediments at Tachibana Bay, located along the western coast of Kyushu, 220 km from the Kikai caldera [Okamura *et al.*, 2005]. A layer of sediments approximately 20 cm thick composed of reworked sand layers, including

granule- and pebble-sized grains, underlies the co-ignimbrite ash layer ascribable to this eruption, with perturbation being interpreted as the result of an energetic tsunami impact [Okamura *et al.*, 2005]. The layer is overlaid by later marine sediments of about 10 m thickness and the depth of the present sea bottom is about 40 m. The sedimentary characteristics and numerical results (wave periods about 10 minutes; Figure 2f) suggested that unidirectional near-bottom currents accompanying tsunamis are sufficient to stir sediment particles into suspension on bases at about 50 m depth. Here, the source conditions of tsunamis, which can stir sediment particles, were investigated using results of numerical calculations. The most widely used criterion for the motion-threshold of sediment particles in water is expressed using the non-dimensional critical boundary shear stress written as $\theta_{cr} = \tau_{cr}/(\sigma - \rho)gd$, where τ_{cr} is the critical boundary shear stress, σ the density of particles, ρ the density of fluid, d the diameter of particles, and g the gravitational acceleration [Allen, 1984].

[14] Assuming a turbulent boundary-layer shear flow for an unidirectional bottom current accompanied with a long wave period tsunami, the boundary shear stress τ can be written as ρU_*^2 , where U_* is the shear velocity at the bottom, and the stress is described as $n\sqrt{gU_0/D}^{1/6}$, using Manning law. $U_0 [= \sqrt{\bar{u}^2 + \bar{v}^2}]$ is the depth-averaged current velocity, which can be directly estimated from the numerical calculations (Table 1 and Figure 2f). In our calculations, U_* was estimated to be less than 0.03 m/s, which is in agreement with the results from the Karman-Prandtle equation [e.g., Furbish, 1997; Noda *et al.*, 2007]. Using these relationships, the non-dimensional boundary shear stress (θ) can be estimated from the equation, $\theta = \tau/(\sigma - \rho)gd$; and the particle motion during the passage of the tsunami can be estimated comparing θ with the Shields criterion (θ_{cr}). Figure 4 is a diagram summarizing the relationship between non-dimensional boundary shear stress for particle entrainment in water and particle size expressed as the particle Reynolds number. The boundary shear stresses for caldera collapse models were calculated using data from Maeno *et al.* [2006], in which tsunami behavior was investigated using non-linear long wave equations and simple-plunger caldera collapse models that show the difference in geometry between pre- and post-collapse (a top of edifice subsiding from +800 or +120 m to -200 or -500 m) and the duration of the collapse (a few tens of seconds to 12 hours). Their results show that with all models the computed tsunami heights were largest when dimensionless collapse speeds (V_c/\sqrt{gh}) were about 0.01. The height substantially decreased with slower speeds (longer collapse durations).

[15] For pyroclastic flow models, θ can not be larger than the threshold values for particle medium-sand size. On the other hand, for the results of caldera collapse models [Maeno *et al.*, 2006], θ can be larger than the threshold values for most of particles, except for long duration-time models. On the basis of these considerations, it is suggested that tsunamis generated by a caldera collapse could easily achieve the boundary shear stress for the threshold values of larger particles, rather than tsunamis generated by a pyroclastic flow entering the sea. Even tsunamis generated by a

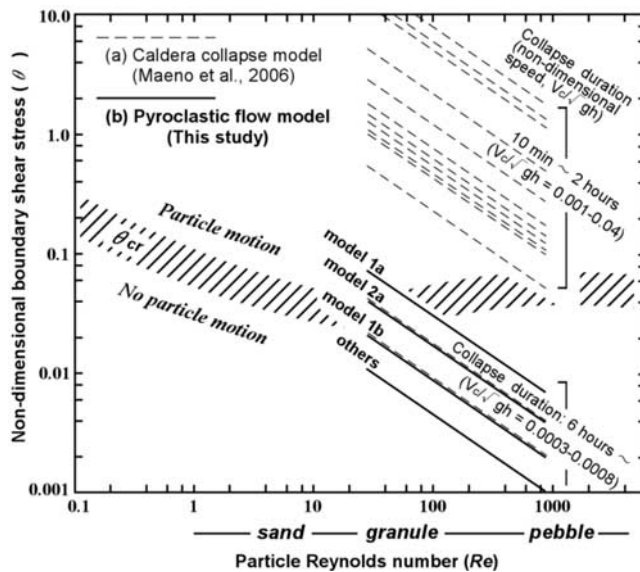


Figure 4. Summary diagrams of the relationship between non-dimensional boundary shear stress (θ) and particle size expressed as the particle Reynolds number (Re), for caldera collapse model (dashed lines) [Maeno *et al.*, 2006] and a pyroclastic flow model (this study, solid lines). The relationship between θ and Re for each tsunami generation model is described as $\theta = f(U_0)/Re$, where $f(U_0)$ is a function of a depth-averaged tsunami velocity (U_0), and the equation makes negative slopes in the log-log plot. A shaded zone indicates the movement threshold (θ_{cr}), called the Shields curve.

large volume flux of such a flow may not have moved the submarine sediments.

7. Summary

[16] Tsunamis, such as the one thought to have been generated by a pyroclastic flow entering the sea during the 7.3 ka Kikai eruption, were examined using non-linear long wave equations with a variable volume flux of a dense component of a pyroclastic flow. Results of numerical computations showed that the maximum height of the tsunami was largest in models with the largest volume flux of the flows ($10^8 \text{ m}^3/\text{s}$). The first positive waves in the larger volume flux models produced run-up on land, but when the volume flux was lower, the tsunami height was drastically decreased to just a few meters and it did not produce run-up in most coastal areas. The approximate volume flux boundary for whether inundation occurs or not was $2 \sim 5 \times 10^7 \text{ m}^3/\text{s}$ at Satsuma Peninsula. The source conditions of a tsunami, which could stir submarine sediments in far areas, were investigated using the non-dimensional boundary shear stress. Numerical results suggested that tsunamis generated by a caldera collapse could easily achieve the shear stress for the threshold values of larger particles rather than a tsunami generated by a pyroclastic flow. During the Holocene explosion of the Kikai caldera, a huge pyroclastic flow occurred and a caldera was formed. Both processes having produced tsunamis, the tsunami generated by the caldera

collapse was the larger and was large enough to affect sand layers in Tachibana Bay.

[17] **Acknowledgments.** We are grateful to H. Taniguchi for critical discussions and comments, and appreciate constructive reviews from two anonymous reviewers. We also thank to JODC (Japan Oceanographic Data Center) and GSI (Geographical Survey Institute of Japan) for providing digital geographical data. This research was partially supported by a Grant-in-aid for Scientific Research 'Dynamics of Volcanic Explosion' from the MEXT.

References

- Allen, J. R. L. (1984), *Sedimentary Structures: Their Character and Physical Basis*, vol. 30, 663 pp., Elsevier, New York.
- Beget, J. E. (2000), Volcanic tsunami, in *Encyclopedia of Volcanoes*, edited by H. Sigurdsson, pp. 1005–1013, Elsevier, New York.
- Carey, S., H. Sigurdsson, C. Mandeville, and S. Bronto (1996), Pyroclastic flows and surges over water: An example from the 1883 Krakatau eruption, *Bull. Volcanol.*, 57, 493–511.
- Cas, R. A. F., and J. V. Wright (1991), Subaqueous pyroclastic flows and ignimbrites: An assessment, *Bull. Volcanol.*, 53, 357–380.
- Furbish, D. J. (1997), *Fluid Physics in Geology*, 476 pp., Oxford Univ. Press, New York.
- Goto, C., and Y. Ogawa (1992), Numerical method of tsunami simulation with the leap-frog scheme, translated from Japanese by N. Shuto, report, Dep. of Civ. Eng., Tohoku Univ., Sendai, Japan.
- Imamura, F., and M. A. Imteaz (1996), Long waves in two-layers: Governing equations and numerical model, *Sci. Tsunami Hazards*, 13, 3–24.
- Japan Coast Guard (1982), Basic map of coastal sea, Satsuma Iwo-jima (in Japanese), scale 1:50000, pp. 1–26, Tokyo.
- Kawamata, K., K. Takaoka, K. Ban, F. Imamura, S. Yamaki, and E. Kobayashi (2005), Model of tsunami generation by collapse of volcanic eruption: The 1741 Oshima-Oshima tsunami, in *Tsunamis: Case Studies and Recent Developments*, edited by K. Satake, pp. 79–96, Springer, New York.
- Machida, H., and F. Arai (1978), Akahoya Ash—A Holocene widespread tephra erupted from the Kikai caldera, south Kyusyu, Japan (in Japanese with English abstract), *Quat. Res.*, 17, 143–163.
- Maeno, F., and H. Taniguchi (2007), Spatiotemporal evolution of a marine caldera-forming eruption, generating a low-aspect ratio pyroclastic flow, 7.3 ka, Kikai caldera, Japan: Implication from near-vent eruptive deposits, *J. Volcanol. Geotherm. Res.*, 167, 212–238.
- Maeno, F., F. Imamura, and H. Taniguchi (2006), Numerical simulation of tsunamis generated by caldera collapse during the 7.3 ka Kikai eruption, Kyushu, Japan, *Earth Planets Space*, 58, 1–12.
- Matsumoto, T., K. Hashi, F. Imamura, and N. Shuto (1998), Development of tsunami generation and propagation model by debris flow (in Japanese), in *Proceedings of 45th Coastal Engineering Conference*, vol. 45, pp. 346–350, Japan Soc. of Civ. Eng., Tokyo.
- McCoy, F. W., and G. Heiken (2000), The Late-Bronze Age explosive eruption of Thera (Santorini), Greece: Regional and local effects, *Geol. Soc. Am. Spec. Pap.*, 345, 43–70.
- McLeod, P., S. Carey, and R. S. J. Sparks (1999), Behaviour of particle-driven flows into the ocean: Experimental simulation and geological implications, *Sedimentology*, 46, 523–536.
- Noda, A., H. Katayama, T. Sagayama, K. Suga, Y. Uchida, K. Satake, K. Abe, and Y. Okamura (2007), Evaluation of tsunami impacts on shallow marine sediments: An example from the tsunami caused by the 2003 Tokachi-oki earthquake, northern Japan, *Sediment. Geol.*, 200, 314–327.
- Okamura, M., H. Matsuoka, and Okamura Makoto Research Committee of Nagasaki Prefecture on Unzen Active Fault System (2005), The evidence of huge Akahoya tsunami recorded in the submarine sediments, 2005 Joint Meeting for Earth and Planetary Science, Japan Geoscience Union, Chiba, Japan.
- Walder, J. S., P. Watts, O. E. Sorensen, and K. Janssen (2003), Tsunamis generated by subaerial mass flows, *J. Geophys. Res.*, 108(B5), 2236, doi:10.1029/2001JB000707.
- Watts, P., and C. F. Waythomas (2003), Theoretical analysis of tsunami generation by pyroclastic flows, *J. Geophys. Res.*, 108(B12), 2563, doi:10.1029/2002JB002265.
- Wohletz, K. H. (1998), Pyroclastic surges and compressible two-phase flow, in *From Magma to Tephra*, vol. 4, edited by A. Freundt and M. Rosi, pp. 247–312, Elsevier, New York.

F. Imamura, Disaster Control Research Center, Graduate School of Engineering, Tohoku University, Aoba, Aoba-ku, Sendai 980-8579, Japan.
F. Maeno, Earthquake Research Institute, University of Tokyo, 1-1-1, Yayoi, Bunkyo-ku, Tokyo 113-0032, Japan. (fmaeno@eri.u-tokyo.ac.jp)